

Compact Printed Four-Element MIMO Antenna System for LTE/ISM Operations

Lingsheng Yang*, Su Yan, and Tao Li

Abstract—A novel four-element multiple-input-multiple-output (MIMO) antenna system for LTE 2300 and 2.45 GHz ISM applications is presented. The total size of the proposed MIMO antenna system is $34\text{ mm} \times 18\text{ mm}$, and the whole antenna system has a wide working bandwidth of 350 MHz (2.19–2.54 GHz). The measured isolation between antenna elements is higher than 15 dB with a close edge-to-edge separation of 0.03λ . Correlation coefficient of the MIMO antenna system is lower than 0.12, which can meet the requirements of 4G wireless systems.

1. INTRODUCTION

The MIMO is a key technology for modern wireless communication standards, such as Long Term Evolution (LTE). In an ideal situation, the increase of the number of transmitter and receiver antennas can improve the communication quality and increase the channel capacity without extra radiation power and spectrum bandwidth [1]. Meanwhile, rapid development of wireless communication devices fulfills the goal of building an ubiquitous society: connecting people anytime and anywhere. As the most important component of these devices, antennas need to have small size, broad bandwidth and easy fabrication [2].

Recently, many printed MIMO antenna systems have been reported. A two microstrip patch antenna array with slotted meander-line resonators for isolation enhancement is reported in [3]. In [4], a modified serpentine structure for mutual coupling reduction in MIMO antennas operating at 2.45 GHz ISM band applications is studied. The antenna elements used in [3, 4] are both microstrip patch antennas. So the size is relatively large, and the bandwidth is narrow. The decoupling structures used in these researches are complicated and space consuming. In [5, 6], two-elements MIMO antenna systems for UWB applications are reported. Fork-like stub and short strip are used to weaken the mutual coupling between elements. Four-element MIMO antenna systems are also developed [7–9]. In [7], the system is designed for a 2.45-GHz ISM band operation, and complementary split-ring resonator (CSRR) loaded on the ground plane is used for antenna miniaturization. System reported in [8] is capable of multiband performance, and the high value of isolation between elements is due to the split in the individual ground plane of each element. Moreover, large size ($58\text{ mm} \times 110\text{ mm}$) and decoupling structures are used in [9].

In this paper, we present a compact four-element planar MIMO antenna system. By using planar monopole as the element, the whole system has a measured -10 dB impedance bandwidth of 350 MHz (2.19–2.54 GHz) with a size of $34\text{ mm} \times 18\text{ mm} \times 1.6\text{ mm}$, only 12.2% of the system reported in [7]. The system can be used for LTE 2300 and 2.45 GHz ISM band applications. Compared to the aforementioned systems [3–9], the proposed four-antenna system does not need any specially designed decoupling structures and has a higher than 15 dB isolation throughout the working band. Correlation coefficients and radiation pattern show that this antenna system is suitable for nowadays portable devices.

Received 8 June 2015, Accepted 1 July 2015, Scheduled 14 July 2015

* Corresponding author: Lingsheng Yang (ylsinchina@163.com).

The authors are with the Jiangsu Key Laboratory of Meteorological Observation and Information Processing, NanJing University of Information Science & Technology, NingLiu Road, Nanjing 210044, China.

2. MIMO ANTENNA DESIGN

The geometry of the proposed MIMO antenna configuration is shown in Figure 1(a). The MIMO antenna, which consists of four planar monopole antenna elements with edge-to-edge separation of 4 mm (0.03λ at 2.19 GHz), was printed on a 1.6 mm thick FR4 substrate with relative permittivity of 4.4 and loss tangent of 0.02. Inspired by the feed structure presented in [8], an uncommon CPW-fed structure proposed in our paper is used to further reduce the mutual coupling and correlation among closely spaced antennas elements. The parameters, such as W_n and W_f , affect the resonant frequency and operation band of the antenna. The curves are shown in Figures 1(d) and (e). The whole length of the path of surface current is around one quarter of the resonant wavelength. The optimal dimensions of the proposed antenna system are as follows:

$L_{sub} = 34$ mm, $W_{sub} = 18$ mm, $W_1 = 1.8$ mm, $W_2 = 2$ mm, $W_3 = 0.6$ mm, $W_4 = 0.9$ mm, $W_f = 0.4$ mm, $W_g = 0.2$ mm, $W_m = 1$ mm, $W_n = 0.2$ mm, $W_p = 4.6$ mm, $L_1 = 5.4$ mm, $L_2 = 4$ mm, $L_3 = 4$ mm, $L_f = 5.5$ mm, $L_g = 7.8$ mm, $L_m = 2.6$ mm, $L_n = 3$ mm.

Compared to the operation frequency (2.19 GHz), the optimized size of the four-element MIMO system is only $0.25\lambda \times 0.13\lambda$. The space between elements is 0.03λ for element1 to element4 and 0.02λ for

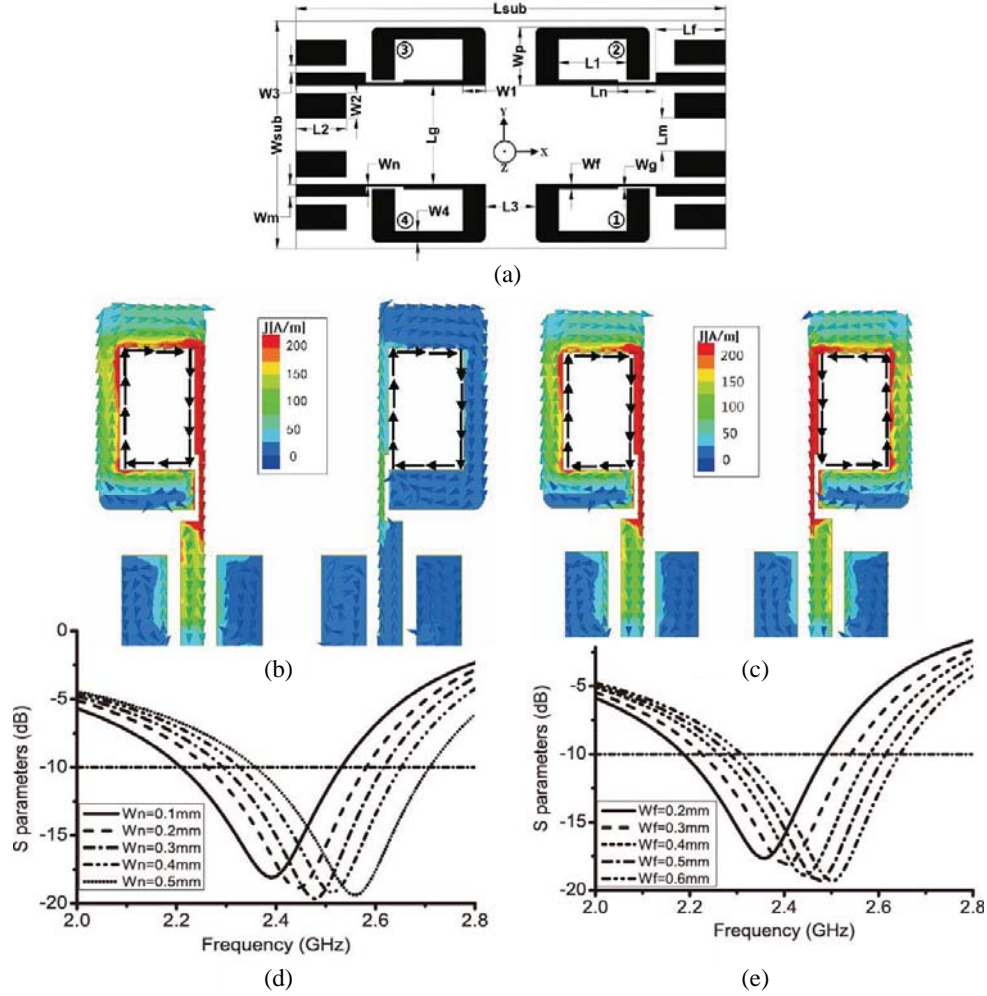


Figure 1. (a) Geometry of the 4-element MIMO antenna system. (b) Simulate surface current distribution on antenna 1 and 2 at 2.45 GHz when only one element is excited. (c) Simulated current distribution on one pair of the elements when both are excited. (d) S parameters with the change of W_n . (e) S parameters with the change of W_f .

Table 1. Comparison between the proposed system and the recently published four-element MIMO antenna systems.

Four-element MIMO system	Size	Bands (GHz)	Isolation (dB)	Space between elements
proposed antenna	$34 \times 18 \times 1.6$ ($0.25\lambda \times 0.13\lambda$)	2.19–2.54	≥ 15	0.03λ
[7]	$100 \times 50 \times 0.8$	2.45 GHz (50 MHz)	10	0.17λ
[8]	$33 \times 36 \times 1.524$	2.28–2.66; 3.35–3.65; 5.07–5.3; 5.75–5.85	14	0.1λ
[9]	$58 \times 110 \times 1.56$	0.734–0.790; 2.307–2.475	4.5	-
[11]	$0.64\lambda \times 0.48\lambda$	2.4–2.5	≥ 25	-

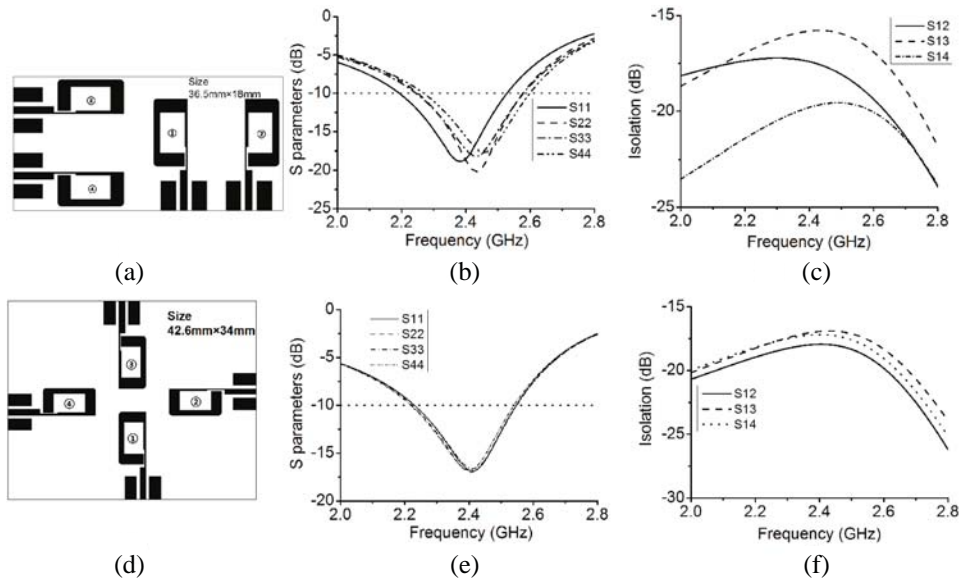


Figure 2. (a) Geometry of type I MIMO antenna system. (b) Simulated reflection coefficients and (c) the simulated isolation for Type I. (d) Geometry of type II MIMO antenna system. (e) Simulated reflection coefficients and (f) the simulated isolation for Type II.

element1 to element2, which is much closer than most of the recently published papers. The comparison between the proposed system and recently published papers with respect of size and performance is listed in Table 1. From the comparison, the proposed antenna has a compact size and acceptable bandwidth and isolation performances.

At frequency higher than megahertz, the current flowing on the surface of a conduct is confined to a relatively small area instead of a uniform distribution due to the well-known skin effect. Therefore, the elements of the proposed MIMO system function as four loop antennas. Figure 1(b) shows the surface currents on the antenna elements when only antenna element1 is excited. Since antenna element2 is the most closely placed element to antenna element1, we mainly focus on the mutual effect between element1 and element2. Although the density of the coupled surface currents on the other three elements is very small, we can still see that the coupled currents rotate and have the same polarization as the excited one.

In Figure 1(c), a pair of antenna elements is excited simultaneously. We can see that the rotation direction of the surface currents is reversed. The two elements act as two opposite polarized loops, which decreases the coupling of one antenna element to the other, and make the system have good isolation without any special designed structure.

When the number of elements increases, size becomes a major limitation. How to maintain a high isolation among antenna elements becomes a challenging task. Therefore, the arrangement of the antenna elements should also be taken into consideration. Figures 2(a), (d) are two different arrangements of the four-elements MIMO systems. The edge-to-edge separations are set to the same as the proposed one. While the elements are orthogonally arranged, the isolation will increase to some degree compared to the proposed system design as shown in (c) and (f). However, the sizes of the MIMO systems are larger than the original one. So the final design of this letter is a compromise between space

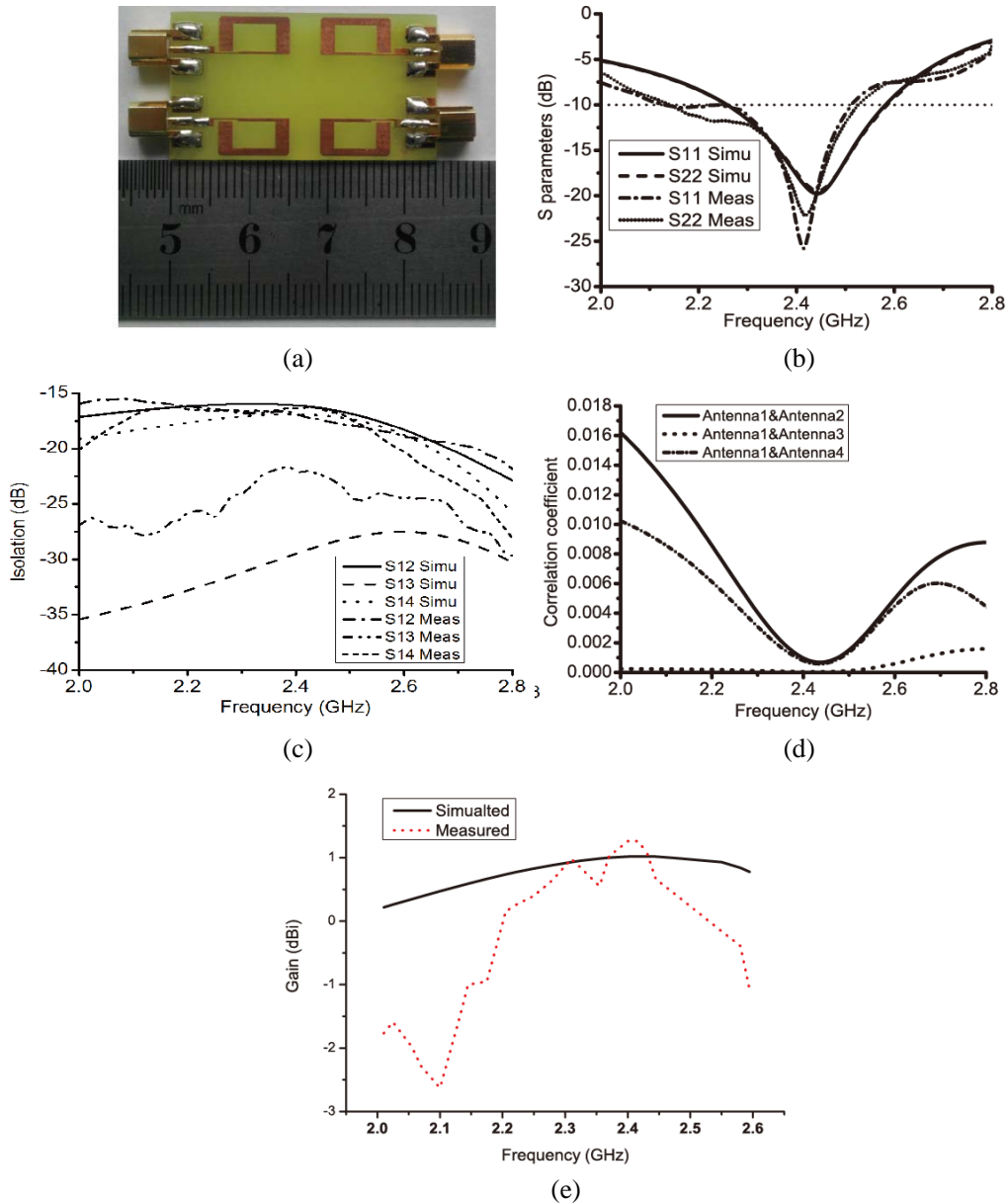


Figure 3. (a) Photograph of fabricated antenna. (b) Reflection coefficients of the MIMO antenna system. (c) Isolation between MIMO antenna elements. (d) Correlation coefficient $|\rho|$ curves for the proposed MIMO antenna system. (e) Gain characteristics of the MIMO antenna system.

and isolation.

Figure 3(a) shows a photograph of the fabricated antenna prototype. The antenna elements were fed by using 50 ohm MCX connectors. The system was measured using Agilent 85058E vector network analyzer.

The measured and simulated $|S_{11}|$ and $|S_{22}|$ of the proposed MIMO antenna configuration are shown in Figure 3(b). $|S_{33}|$ and $|S_{44}|$ are not shown because the four antenna elements are symmetrical. According to the simulation, the antenna has a 340 MHz (2.24–2.58 GHz) bandwidth, while the measured results of the 10 dB return loss bandwidth is 350 MHz (2.19–2.54 GHz). The differences between the measured and simulated values are probably caused by fabrication imperfections and the loss of feeding cable and connectors. The measured operation bandwidth shows that this MIMO antenna system is suitable for LTE 2300 and 2.45 GHz ISM applications.

The measured isolation among antenna elements is shown in Figure 3(c). Through the whole working band, the isolation is higher than 15 dB, which fits the requirement of well accepted standards for MIMO antenna system [11].

The correlation coefficient is an important parameter for an MIMO antenna system, which can be calculated from the measured S parameters, and it is given by [10]

$$|\rho_{ij}| = \left| \frac{|S_{ii}^* S_{ij} + S_{ji}^* S_{jj}|}{\sqrt{(1 - |S_{ii}|^2 - |S_{ji}|^2)(1 - |S_{jj}|^2 - |S_{ij}|^2)} \eta_{radi} \eta_{radj}} \right| \quad (1)$$

Figure 3(d) shows the correlation coefficient between the antenna elements of the proposed MIMO

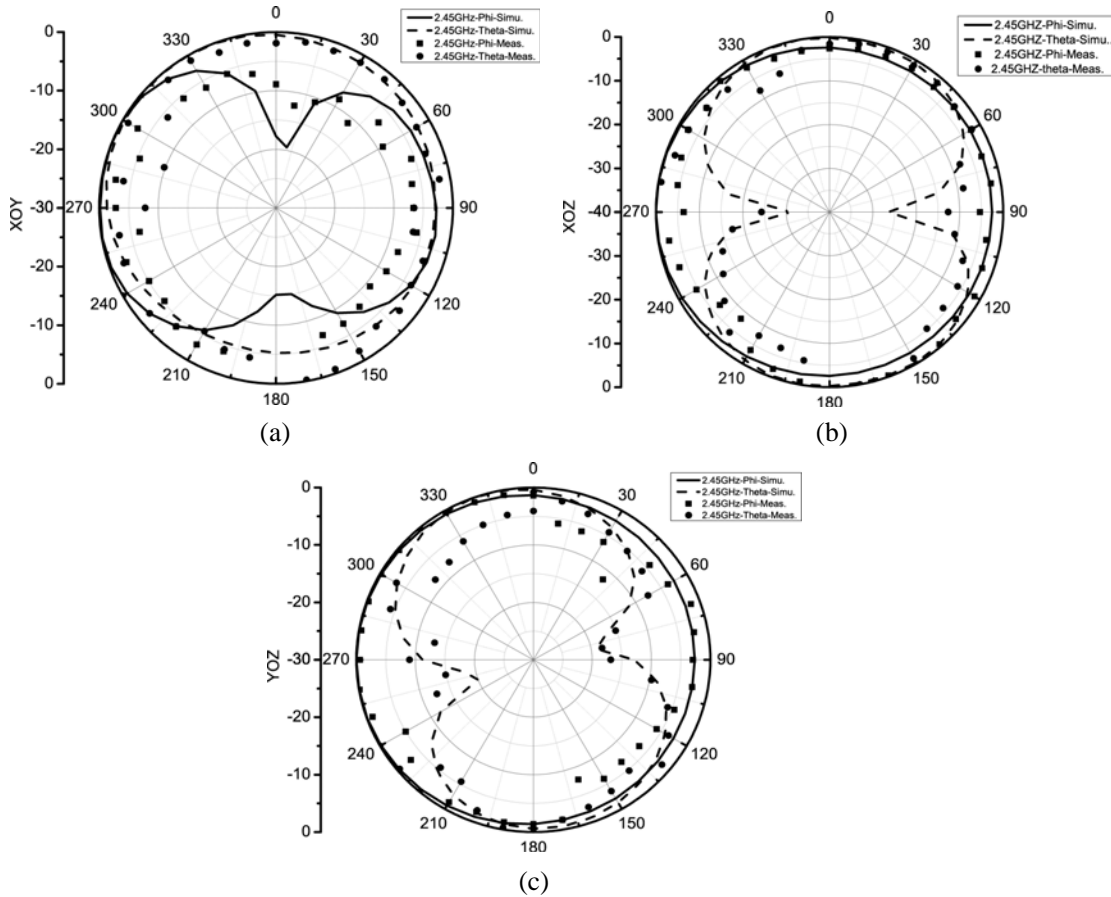


Figure 4. Radiation patterns of the proposed antenna: (a) xy -plane, (b) xz -plane, (c) yz -plane.

antenna system. The antenna efficiency used here is $\eta = 78\%$. The maximum value of the correlation coefficient is far below 0.3, which is the maximum value set for 4G standards [7].

The simulated and measured gains of the antenna system versus frequency are shown in Figure 3(e). Within the frequency range from 2.19 to 2.54 GHz, the simulated gains are about 0.8 dBi with 0.3 dBi variation. The measured gain varies from 0.13 dBi to 1.26 dBi, and the peak measured gain is 1.26 dBi at 2.4 GHz.

The radiation patterns of antenna element1 in xy -, yz - and xz -planes at 2.45 GHz are shown in Figure 4, while the other three antenna elements are terminated with a 50 ohm load. The radiation patterns of other three antenna elements are not shown here because of the symmetry among antenna elements.

In practical application, antennas are always integrated with other electronic devices, and they usually share a common ground. In Figure 5(a), the MIMO antenna system was placed above a ground plane separated by free space. The separation between the conductive board and antenna bottom side was varied from 1 to 5 mm in 1-mm steps. Figure 5(b) shows the reflection coefficients of antenna element over a metal sheet at different distances. It was found that when the board is closely placed under the system such as 1 mm, the resonant frequency is shifted, but the working band can still cover the aforementioned bands. As the distance between the antenna and conductive plane is increased, the effect of the conductive plane weakens. Figure 5(c) shows the isolation among antenna elements over a metal sheet at 1 mm. The performance of the antenna system does not change much, unlike the system

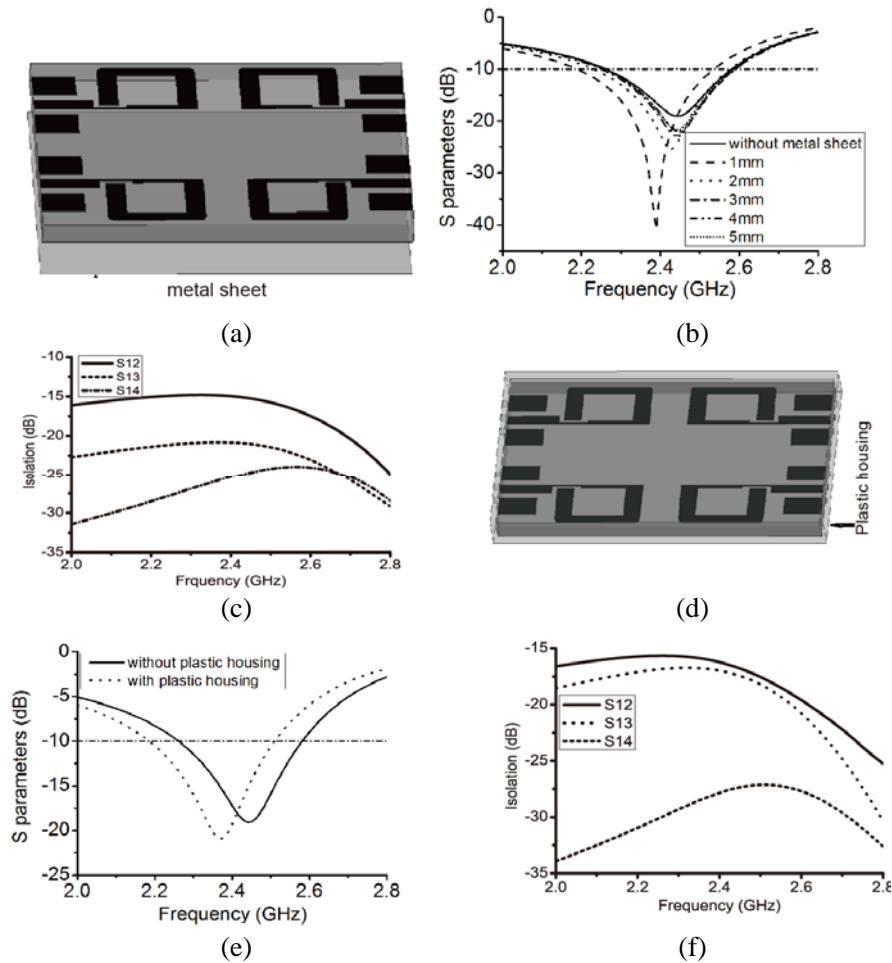


Figure 5. (a) Proposed MIMO antenna with a ground plane separated by free space. (b) Reflection coefficients of the MIMO antenna system with metal sheet. (c) Isolation characteristics. (d) Proposed antenna with plastic housing. (e) Reflection coefficients. (f) Isolation characteristics.

reported in [7], and the antenna system was not strongly affected by the distance from the conductive board to its bottom side and is convenient for practical design.

Figure 5(d) shows a 0.5 mm thick plastic housing around the MIMO system to simulate the practical case of the wireless terminals. In simulation, the relative permittivity of the plastic housing is set at 3.3, and the loss tangent is 0.02. Figures 5(e), (f) show the influence of the plastic housing on S parameters. Differences between the two cases are acceptable and show that this MIMO system is competitive for practical application.

3. CONCLUSION

A four-element MIMO antenna system for LTE and ISM application is proposed. The antenna system covers 2.19–2.54 GHz band with a total size of 34 mm \times 18 mm \times 1.6 mm. Without any special designed decoupling structure, the isolation among antenna elements is more than 15 dB. The characteristics of the whole antenna system do not change much when integrated with a plastic case. Antenna efficiency, correlation coefficient and radiation performance make it suitable for nowadays wireless devices.

ACKNOWLEDGMENT

This work was supported by the Priority Academic Program Development of Jiangsu Higher Education Institutions (PAPD).

The authors would like to thank Professor Hongting Jia of Kyushu University, Japan, for his patient discussion on this paper.

REFERENCES

1. Song, L. and J. Shen, *Evolved Cellular Network Planning and Optimization for UMTS and LTE*, CRC Press, London, 2011.
2. Chen, Z. N. and M. Y. W. Chia, *Broadband Planar Antennas: Design and Applications*, Wiley, 2006.
3. Alsath, G., M. Kanagasabai, and B. Balasubramanian, "Implementation of slotted meander-line resonators for isolation enhancement in microstrip patch antenna arrays," *IEEE Trans. Antennas Propag.*, Vol. 12, 15–18, 2013.
4. Arun, H., A. K. Sarma, M. Kanagasabai, S. Velan, C. Raviteja, and M. G. N. Alsath, "Deployment of modified serpentine structure for mutual coupling reduction in MIMO antennas," *IEEE Trans. Antennas Propag.*, Vol. 13, 277–280, 2014.
5. Gao, P. and S. He, "A compact UWB and Bluetooth slot antenna for MIMO/diversity applications," *ETRIJ*, Vol. 36, No. 2, 309–312, Apr. 2014.
6. Liu, L., S. W. Cheung, and T. I. Yuk, "Compact MIMO antenna for portable devices in UWB applications," *IEEE Trans. Antennas Propag.*, Vol. 61, No. 8, 4257–4264, 2013.
7. Sharawi, M. S., M. U. Khan, A. B. Numan, and D. N. Aloï, "A CSRR loaded MIMO antenna system for ISM band operation," *IEEE Trans. Antennas Propag.*, Vol. 61, No. 8, 4265–4274, 2013.
8. Karimian, R., H. Oraizi, S. Fakhte, and M. Farahani, "Novel F-shaped quad-band printed slot antenna for WLAN and WiMAX MIMO systems," *IEEE Antennas and Wireless Propagation Letters*, Vol. 12, 405–408, 2013.
9. Sharawi, M. S., M. A. Jan, and D. N. Aloï, "Four-shaped 2 \times 2 multi-standard compact MIMO antenna system for long-term evolution mobile handsets," *IET Microw. Antennas Propag.*, Vol. 6, No. 6, 685–696, 2012.
10. Blanch, S., J. Romeu, and I. Corbella, "Exact representation of antenna system diversity performance from input parameter description," *Electron. Lett.*, Vol. 39, No. 9, 705–707, 2003.
11. Li, H., J. Xiong, and S. L. He, "A compact planar MIMO antenna system of four elements with similar radiation characteristics and isolation structure," *IEEE Antennas and Wireless Propagation Letters*, Vol. 8, 1107–1110, 2009.